HHS Public Access

Author manuscript

Neuron. Author manuscript; available in PMC 2017 September 07.

Published in final edited form as:

Neuron. 2016 September 7; 91(5): 1034–1051. doi:10.1016/j.neuron.2016.07.002.

Expression of C1ql3 in Discrete Neuronal Populations Controls Efferent Synapse Numbers and Diverse Behaviors

David C. Martinelli[1,*], **Kylie S. Chew**[2], **Astrid Rohlmann**[3], **Matthew Y. Lum**[1], **Susanne Ressl**[1,4], **Samer Hattar**[2], **Axel T. Brunger**[1,5], **Markus Missler**[3], and **Thomas C. Südhof**[1,5]

[1]Dept. of Molecular and Cellular Physiology, Stanford University School of Medicine, Stanford CA 94305, USA

[2]Dept. of Biology, The Johns Hopkins University, Baltimore, MD 21218, USA

[3]Institute of Anatomy and Molecular Neurobiology, Westfälische Wilhelms Universität, Münster, Germany

[4]Dept. of Molecular and Cellular Biochemistry, Indiana University, Bloomington, IN 47405 USA

[5]Howard Hughes Medical Institute, Stanford University School of Medicine, Stanford CA 94305, USA

Abstract

C1ql3 is a secreted neuronal protein that binds to BAI3, an adhesion-class GPCR. C1ql3 is homologous to other gC1q-domain proteins that control synapse numbers, but a role for C1ql3 in regulating synapse density has not been demonstrated. We show in cultured neurons that *C1ql3* expression is activity-dependent and supports excitatory synapse density. Using newly generated conditional and constitutive *C1ql3* knockout mice, we found that *C1ql3*-deficient mice exhibited fewer excitatory synapses and diverse behavioral abnormalities, including marked impairments in fear memories. Using circuit-tracing tools and conditional ablation of *C1ql3* targeted to specific brain regions, we demonstrate that *C1ql3*-expressing neurons in the basolateral amygdala project to the medial prefrontal cortex, that these efferents contribute to fear memory behavior, and that *C1ql3* is required for formation and/or maintenance of these synapses. Our results suggest that C1ql3 is a signaling protein essential for subsets of synaptic projections and the behaviors controlled by these projections.

eTOC blurb

[*]Address for correspondence at martinelli@stanford.edu.

AUTHOR CONTRIBUTIONS

Conceptualization and Methodology, DCM, KSC, and TCS; Investigation, DCM, KSC, AR, MYL, MM; Writing – Original Draft, DCM, and TCS; Writing – Review & Editing, DCM, KSC, MYL, SR, MM, and TCS; Visualization, DCM; Supervision, SH, ATB, TCS.

Synapses impact every moment of our subconscious and conscious mind but the genes that control their organization are mostly mysterious. Martinelli et al. show here that the *C1ql3* gene promotes synapse maintenance in brain and contributes to the formation of emotionally salient memories.

INTRODUCTION

The importance of synapses cannot be overstated as their collective activities impact every moment of our subconscious and conscious mind. In brain, synapses are formed and continuously restructured throughout life with an amazing specificity and activity-dependent plasticity based on our different experiences, which ultimately shapes us as individuals with unique memories, thoughts, skills, and personalities. How synapses are organized so precisely remains largely unknown. In the present study, we explored the potential role of C1ql proteins as synaptic organizers that contribute to the formation and/or function of a selected set of synapses. C1ql proteins (for 'complement component 1, q subcomponent-like') are encoded by four homologous genes that are primarily expressed in brain (*C1ql1-4*). C1ql's are composed of an N-terminal signal peptide followed by a short sequence with conserved cysteines, a collagen-like region, and a C-terminal globular C1q domain (gC1q; Fig. 1A) (Ghai et al., 2007). gC1q domains assemble into obligate trimers; C1ql's and other gC1q-domain proteins further multimerize via N-terminal domains into higher molecular weight oligomers. Among gC1q-domain proteins, C1ql's most resemble C1q's, cerebellins, and adiponectin (Fig. 1A) (Caselli, 2014; Hirai et al., 2005; Stevens et al., 2007). Recent crystallographic analyses revealed that despite their sequence similarities, C1ql's have unique electrostatic surface properties compared to other gC1q-domain proteins, suggesting that C1ql's have specific binding partners (Ressl et al., 2015). C1ql3 is the most broadly expressed C1ql isoform, and is highly conserved evolutionarily with only a single aminoacid change between human and mouse (Iijima et al., 2010).

Our initial experiments suggested that C1ql's may function in synapse elimination and/or maintenance (Bolliger et al., 2011), and elegant recent studies confirmed a synaptic role for C1ql1 in the cerebellum (Kakegawa et al., 2015; Sigoillot et al., 2015). Furthermore, we identified C1ql proteins as high-affinity ligands for BAI3 (renamed ADGRB3 (Hamann et al., 2015)), an adhesion-class GPCR, which was validated as a C1ql1 receptor in cerebellum (Bolliger et al., 2011; Kakegawa et al., 2015). When expressed in neurons, BAI3 is localized postsynaptically and influences excitatory synapse formation and/or maintenance, perhaps by regulating actin dynamics in dendrites (Kakegawa et al., 2015; Lanoue et al., 2013). Consistent with an important function for C1ql's and BAI3 in brain, single nucleotide polymorphisms in *BAI3* significantly associate with predisposition to schizophrenia and addiction in genome-wide association studies (DeRosse et al., 2008; Liu et al., 2006).

In the present study, we found that *C1ql3* is broadly expressed throughout the brain, but only in discrete subsets of neurons, including excitatory projection neurons of the basolateral amygdala (BLA) and the insular and perirhinal cortices. The amygdala is a critical component for learning of rewarding and fearful stimuli, and contains multiple subdivisions (Duvarci and Pare, 2014). The BLA subdivision sends projections to multiple other brain structures, including the nucleus accumbens (NAc), hippocampus, and medial prefrontal

cortex (mPFC) (Janak and Tye, 2015). The projection from the BLA to the mPFC is particularly interesting because it is critical for both learning and extinction of fear memories (Duvarci and Pare, 2014). Enormous progress recently led to a sophisticated understanding of the general role of the BLA (Janak and Tye, 2015), but little is known about the molecular basis for the formation of output synapses from the BLA.

Here, we show in cultured neurons that *C1ql* expression is upregulated in concert with excitatory synaptogenesis, and that *C1ql's* promote excitatory synapse density. To address the function of C1ql3, we generated and analyzed constitutive and conditional *C1ql3* knockout (KO) mice. We found that constitutive ablation of *C1ql3* produced diverse behavioral changes, including hyperactivity, impairments in motor learning, and a deficit in association learning of rewarding and aversive stimuli. We found that conditional inactivation of *C1ql3* in the BLA by stereotactic viral manipulations reproduced the fear memory impairment detected in constitutive *C1ql3* KO mice. Consistent with a role for *C1ql3* in amygdala fear circuits, we further demonstrate that *C1ql3*-positive neurons in the BLA form synaptic projections to the mPFC, that *C1ql3* is required for these synaptic projections, and that these C1ql3-dependent synapses contribute to fear memory behavior. Moreover, we observed that *C1ql3* KO mice exhibited a reduced excitatory synapse density in the specific mPFC subregions innervated by *C1ql3*-positive BLA neurons. Viewed together, our data suggest that C1ql3 is a novel synaptic organizing molecule required for a subset of synaptic connections that are centrally involved in key behaviors.

RESULTS

C1ql proteins promote excitatory synapse density in cultured neurons

We previously observed that addition of the purified recombinant gC1q domain from C1ql proteins to cultured neurons decreased their excitatory synapse density (Bolliger et al., 2011), suggesting that C1ql proteins may control synapse formation and/or maintenance. To directly test this hypothesis, we constructed a lentivirus expressing an shRNA that simultaneously targets *C1ql1–3* (*C1ql4* expression was undetectable in cultured forebrain neurons). mRNA measurements validated that the shRNA efficiently decreased expression of *C1ql1–3* to <12% of controls (Fig. S1A). We also created an overexpression lentivirus to produce C1ql3 under control of the ubiquitin promoter, and a 'rescue' lentivirus that expressed both the shRNA and C1ql3 protein.

We found that knockdown of *C1ql's* in cultured hippocampal neurons caused a decrease in excitatory synapse density as determined by immunofluorescence for VGluT1, an excitatory presynaptic marker (Fig. 1B). The *C1ql* RNAi also prevented the increase in synaptogenesis that normally occurs after a 3-day treatment with tetrodotoxin (TTX) (Arendt et al., 2013), suggesting that C1ql proteins contribute to homeostatic scaling in response to activity blockade. We observed no change in either the mean size of synaptic puncta or their mean fluorescence intensity, suggesting that the morphological properties of the remaining synapses were unchanged (Fig. S1B). Moreover, we detected no change in inhibitory synapse numbers as determined by immunofluorescence for VGAT, an inhibitory presynaptic marker, consistent with the notion that *C1ql* specifically promotes excitatory synapse formation and/or maintenance.

This conclusion seemingly is at odds with our previous experiment showing that addition of the recombinant gC1q domain from C1ql proteins caused a reduction in excitatory synapse density (Bolliger et al., 2011) comparable to the C1ql knockdown. However, our previous experiments exogenously applied truncated C1ql proteins, which may have created a dominant-negative effect. To further support a positive role for C1ql proteins at synapses, we examined the activity-dependence of *C1ql* expression. We observed that a three-day period of activity blockade with TTX or with NBQX and d-APV (AMPA- and NMDA-receptor antagonists, respectively) caused an increase in *C1ql1–3* expression, consistent with a synapse promoting role of C1ql's (Fig. 1C). NBQX alone or picrotoxin (a $GABA_A$-receptor blocker) had no effect. We conclude from these experiments that *C1ql* genes promote excitatory synapse density in cultured neurons, and exhibit an increase in expression upon synaptic silencing.

C1ql3 is expressed in specific brain regions, such as the BLA and insular cortex

qRT-PCR measurements of the relative expression of *C1ql1–4* in various brain regions dissected from adult mice revealed that *C1ql3* was broadly expressed in many brain regions, including all cortical areas tested, whereas *C1ql1* was detected at a low level in most brain regions except for the hindbrain, and *C1ql2* was only expressed highly in the hippocampus (Fig. S1C). Because of its broad expression, we decided to focus on *C1ql3*. We used homologous recombination in embryonic stem cells to generate *C1ql3* conditional KO (cKO) mice. In the *C1ql3* cKO allele (*C1ql3*^{flox}), the second and final *C1ql3* exon was floxed and an IRES-mVenus sequence was inserted into the 3′ UTR, which marks *C1ql3*-expressing cells and is inactivated by Cre-recombinase together with excision of the exon (Fig. 1D).

To determine which cell types express *C1ql3*, we performed double immunofluorescence analyses for mVenus and various markers in cultured cortical neurons and in cryosections of brains from *C1ql3*$^{flox/flox}$ mice. We observed mVenus co-localization with the pan-neuronal markers MAP2 and Hu, and with the excitatory neuronal marker CaMKIIα, but not with the inhibitory neuronal marker GAD67 (Fig. S1D, S1E). Depending on which region of cortex was cultured, the fraction of mVenus-positive excitatory neurons ranged from 25%–50%, demonstrating that only a subset of neurons express C1ql3. We also observed a small number of unidentified cells that expressed mVenus that could represent glia. Overall, these results indicate that *C1ql3* is predominantly expressed in a subset of excitatory neurons.

Analysis of mVenus localization on sagittal and coronal cryosections of adult *C1ql3*$^{flox/flox}$ mice revealed a distinctive expression pattern. *C1ql3*/mVenus-expressing neurons were prominent in the dentate gyrus (DG; Fig. 2A, 2B, 2E, 2F), the BLA (Fig. 2B, 2E), and the retrosplenial, piriform (Pir), and entorhinal cortices (EntRh; Fig. 2B, 2E, 2F, S2A). In addition, strong mVenus localization was observed throughout the anterior/posterior length of the insular cortex (Fig. 2B, 2C and S2A, S2B), and appeared particularly enriched in the agranular part of the insular cortex (Fig. S2C). mVenus expression was consistently present proceeding posteriorly from the insular cortex along the transitional area between the ventrally adjacent allocortex and the dorsally adjacent neocortex, as the agranular insular cortex transitions into the agranular perirhinal cortex (PRh; Fig. 2E, 2F, and S2A). In the

prefrontal cortex, as in other cortical regions, mVenus was observed in cortical layer 1, likely reflecting *C1ql3*-expressing local neurons as well as incoming projections from other *C1ql3*-expressing neurons (Fig. 2C, 2D). Moreover, the *C1ql3* knockin allele allowed detection of mVenus-positive axonal projections, such as the mossy fibers emanating from the dentate gyrus (Fig. 2G) and the stria terminalis, an output fiber bundle of the amygdala (ST; Fig. 2E). Despite little mRNA expression (Fig. S1C), the olfactory bulb granule cell layer (GrO), the central amygdala (Ce), and the entire striatum contained detectable mVenus protein, suggesting that *C1ql3*-expressing neurons project into these areas (Fig. 2A, 2B, 2E, S2B).

C1ql3 is presynaptically localized

Expression of the $C1ql3^{flox}$ allele in dentate gyrus granule cells caused production of mVenus that was transported down axons to presynaptic mossy fiber terminals in the stratum lucidum of the CA3 region (Fig. 2G top). To test whether C1ql3 protein itself was transported into nerve terminals similar to C1ql1 protein in cerebellum (Hirai et al., 2005), we performed immunofluorescence labeling for C1ql3. C1ql3 was strongly enriched in presynaptic terminals; the C1ql3 signal was ablated in *C1ql3* KO mice, demonstrating its specificity (Fig. 2G, bottom 2 rows). In addition, we expressed HA-epitope tagged C1ql3 in cultured neurons using the lentivirus described above, and observed that HA-tagged C1ql3 was localized to presynaptic terminals (Fig. S2D). We conclude that C1ql3 is likely localized to presynaptic terminals.

Constitutive *C1ql3* KO causes multiple behavioral impairments

We converted $C1ql3^{flox/flox}$ mice into constitutive *C1ql3* KO mice using germline expression of Cre-recombinase. Homozygous *C1ql3* KO ($C1ql3^{-/-}$) mice contained no detectable C1ql3 or mVenus protein (Fig. S3A, S3B), but were viable and fertile, bred in the expected Mendelian ratio, and exhibited a normal body weight (Fig. 3A, 3B). *C1ql1* and *C1ql2* were not up-regulated in neocortex from homozygous *C1ql3* KO mice (Fig. S3C). Thus, *C1ql3* is not essential for mouse survival or breeding.

We next performed a battery of behavioral tests on littermate wild-type, hetero- and homozygous *C1ql3* KO mice. *C1ql3* KO mice displayed normal acoustic startle responses, sensorimotor gating in the prepulse inhibition assay, and social interactions (Fig. 3C, S3D, S3E). However, homozygous *C1ql3* KO mice exhibited a modest motor learning deficit in the accelerating rotating rod assay (Fig. 3D), and both homo- and heterozygous *C1ql3* KO mice were hyperactive in the open field and displayed apparently decreased anxiety in the elevated plus maze (Fig. 3E, 3F).

C1ql3 is expressed in several brain areas that play critical roles in learning and memory, including the hippocampus, amygdala, and cortical areas, such as the perirhinal cortex and mPFC. To examine the role of *C1ql3* in learning and memory, we tested fear conditioning, a classical paradigm to measure associative learning. In this experiment (Fig. 3G), foot shocks are paired on day 1 with a particular spatial context in the experimental chamber and with an acoustic signal (a tone); when the mouse is returned to the chamber on day 2 (no tone presented), memory of the chamber context is assayed by quantifying the fear-induced freezing response. On day 3, finally, the context of the chamber is modified to be distinct

from the original to measure freezing in an altered but similar context, and the mouse is assayed for cued fear memory by monitoring freezing in response to the tone.

Both hetero- and homozygous *C1ql3* KO mice displayed reduced freezing in the standard context test on day 2 (Fig. 3H). In addition, mutant mice exhibited less freezing in the 1 min observation period immediately after the last foot shock on day 1, suggesting a possible short-term or working fear memory deficit. Interestingly, the mutant mice displayed a normal reduction in freezing in the altered context on day 3, and exhibited a normal freezing response to the tone, suggesting that for at least the 2 day memory test, *C1ql3* only contributes to contextual fear memory.

Given the strong expression of *C1ql3* in the insular cortex and the relation of this brain region to drug addiction and reward (Naqvi and Bechara, 2010), we performed cocaine-conditioned place preference (CPP) experiments with various cocaine concentrations (Fig. 3I). CPP is a form of Pavlovian conditioning that is routinely used to measure the rewarding effects of objects or experiences (*e.g.* abused drugs), and also requires intact contextual memory (Bardo and Bevins, 2000). Mice were first habituated to a chamber with a different context (distinct textured/colored floors) in each half, and subsequently conditioned to associate one context with the effects of cocaine. On the preference test day, mice were allowed to choose which zone of the chamber to occupy. Wild-type and heterozygous *C1ql3* KO mice displayed robust preference for the cocaine-associated context, starting at a dose of 10 mg/kg. In contrast, homozygous *C1ql3* KO mice seemed to have no memory of the context (Fig. 3J). Nevertheless, mutant and wild-type mice exhibited the same cocaine-induced increase in locomotion and movement velocity, suggesting that the *C1ql3* KO does not impair the animals' immediate physiological response to cocaine (Fig. 3K, S3G). Moreover, in a separate cohort of mice, cocaine sensitization after daily injections was independent of *C1ql3* genotype (Fig. S3F).

In the next experiments, we tested conditioned place aversion (CPA) by pairing a particular context with a malaise-inducing lithium injection. The homozygous *C1ql3* KO also blocked place-associated memory in the CPA paradigm (Fig. 3L). Since in CPA the memory is associated with a negative experience, the loss of a response in the CPP paradigm (Fig. 3J) was not specific for rewards. Analogous to the cocaine response, *C1ql3* KO mice similar to control mice displayed decreased locomotion and movement velocity in response to lithium – in fact, the distance traveled was slightly lower in *C1ql3* KO mice even though they are hyperactive (Fig. 3M, S3H).

The overall picture that emerges from these behavioral studies is that *C1ql3* KO mice are hyperactive and exhibit a marked impairment of emotionally marked contextual memories. To test whether *C1ql3* KO mice exhibit a general memory deficit, we performed three additional behavioral tests which measure different types of memory, namely novel object recognition, Y-maze (working memory), and the Morris water maze (spatial memory; Fig. 3N–P). We detected no phenotypic change in any of these diverse tests, suggesting normal declarative and spatial memory. C1ql3 is abundantly present in the hippocampus, but compensation by C1ql2 seems likely since *C1ql2* and *C1ql3* appear to be co-expressed in the same dentate gyrus granule neurons (Fig. S1C and (Iijima et al., 2010)).

We conclude from our behavioral analysis that the *C1ql3* KO produces a diverse set of behavioral phenotypes, including hyperactivity, reduced motor learning, and an apparent decrease in anxiety. Additionally, the fear conditioning, CPP, and CPA phenotypes could be grouped together to suggest that the mutants have a deficit in associating emotionally salient stimuli with discrete contexts. It is not immediately clear why heterozygous KO mice resemble wild-type mice in some assays and homozygous KO mice in others. Possibly *C1ql3* expressed in distinct brain regions regulates different behaviors, and *C1ql3* haploinsufficiency may produce a functional impairment in some but not all of these brain regions.

C1ql3 expression in the BLA is required for normal fear memories

To identify the specific brain regions responsible for some of the observed behavioral phenotypes, we produced three adeno-associated viruses (AAVs) for regional manipulation of C1ql3 expression in cKO mice, namely AAVs expressing (i) mutant Cre-recombinase and mCherry separated by a P2A peptide (ΔCre-mCherry, as a control), (ii) wild-type Cre-recombinase alone (Cre), and (iii) wild-type Cre-recombinase together with rescue C1ql3 protein (Cre-IRES-C1ql3). All protein expression was driven by the neuron-specific synapsin promoter. The AAVs functioned as expected as determined by qRT-PCR in pilot experiments with cultured neurons from cKO mice (Fig. S4A).

We initially chose to target the posterior insular cortex with stereotaxic AAV injections into adult cKO mice (Fig. 4A). Although the AAVs were accurately targeted to the posterior insula, the relatively large amounts of AAVs used in these experiments also infected the anterior BLA and perirhinal cortex that are close to the injection site (Fig. 4B). After more than 4 weeks post-surgery, mice were tested behaviorally. We found that Cre expression in the insular cortex/perirhinal cortex/BLA significantly impaired contextual fear memories, but surprisingly had no effect on CPP or other assayed behaviors (Fig. 4C–4G, S4B-S4F). The fear memory phenotype was not detected after expression of ΔCre or Cre-IRES-C1ql3, demonstrating specificity.

Based on these results, we asked whether the contextual fear memory phenotype we observed may be solely due to deletion of *C1ql3* from the BLA, which is central for fear memory formation, and/or the perirhinal cortex which is also involved in memory formation. We tested this question by separate stereotactic injections of AAVs expressing wild-type or mutant Cre into the BLA and perirhinal cortex. Injections targeting the perirhinal cortex yielded no phenotype (Fig. S4I–S4N). Gratifyingly, injections targeting the BLA replicated the loss of contextual fear memory of constitutive *C1ql3* KO mice without causing any other behavioral phenotype as far tested (Fig. 4H–4N, S4G, S4H).

It is intriguing that constitutive deletion of *C1ql3* and conditional deletion of *C1ql3* only from the BLA, selectively impair contextual but not cued fear memory as examined 48 hours after training, as both forms of learning involve BLA activation. We therefore tested the conditional mutants for cued fear memory again 4 weeks post-training and observed a significant decrease in freezing in mice with *C1ql3* inactivation in the BLA (Fig. 4J). It is unclear from these experiments whether the *C1ql3* deletion in the BLA renders cued fear memory less stable or promotes active memory extinction. Alternatively, cued fear memory

may be significantly more robust than contextual fear memory in our experimental apparatus. Regardless, these data show that the function of C1ql3 in the BLA is not restricted to contextual fear memories. We conclude that *C1ql3* expressed specifically in the BLA has an important role in Pavlovian fear memory, and that the population of *C1ql3*-expressing neurons in the BLA is distinct from the *C1ql3*-expressing neurons which modulate CPP, CPA, hyperactivity, motor learning, and elevated plus maze behaviors.

C1ql3-expressing neurons of the BLA project to the mPFC and NAc

How does *C1ql3* act in the BLA? Approximately half of anterior BLA neurons express C1ql3, raising the question of whether these neurons project to specific brain regions, and whether C1ql3 might be involved in forming and/or maintaining synaptic projections from the BLA to these brain regions. Since C1ql3 is transported to presynaptic terminals, their projection targets may identify synapses that are responsible for fear memory behaviors. Prior analyses using microarray expression profiling of the commonly used *Thy1-Yfp-H* transgenic line showed that YFP-positive cells in the amygdala are glutamatergic projection neurons that specifically express *C1ql3* (Feng et al., 2000; Sugino et al., 2006). It was noted that the *Thy1-Yfp-H* expression in the BLA was greater in the anterior BLA and lower in the posterior BLA. Furthermore, mapping of the *Thy1-Yfp-H* expression pattern revealed that labeled axons exit the BLA along the stria terminalis and project to the NAc, olfactory tuberculum, and also likely to the mPFC (Porrero et al., 2010). This expression pattern is consistent with our observations of *C1ql3*/mVenus localization.

Motivated by this information, we performed circuit-tracing studies using a recombinant rabies virus that expressed tdTomato (Lim et al., 2012). Rabies virus is taken up at presynaptic terminals and retrogradely transported to the soma, but cannot spread to other neurons. We injected recombinant rabies virus into the mPFC of *Thy1-Yfp-H* mice, and confirmed the predicted projection of *Thy1-Yfp-H*-positive BLA neurons to the mPFC (Fig. S5A, S5B). Next, we injected rabies virus into the dorsal striatum, NAc, and multiple locations of the mPFC in $C1ql3^{flox/flox}$ mice and determined where in brain the mVenus and tdTomato markers co-localize.

We found no *C1ql3*-positive projections from the BLA to the dorsal striatum, but significant *C1ql3*-positive projections from the BLA to the mPFC via the stria terminalis. In the mPFC, rabies virus injections targeting the infralimbic cortex (ILC) (which also partially infected the prelimbic cortex [PLC]) caused production of abundant tdTomato-positive neurons in the BLA, of which ~72% were clearly also *C1ql3*-positive (Fig. 5A–E). Approximately 4% of the total *C1ql3*-positive BLA neurons also expressed tdTomato, although the overall fraction of *C1ql3*-positive BLA neurons that project to the PFC is likely higher, as the efficiency of the rabies virus is not 100% and the injection only targeted a portion of the PFC. Additional rabies virus injections targeting the prelimbic cortex or the cingulate cortex showed that 60% and 39%, respectively, of tdTomato-positive neurons in the BLA were also *C1ql3*-positive (Fig. S5C–S5F). We also observed *C1ql3*-positive BLA neurons projecting to the NAc core, with ~27% of the BLA neurons that project to the NAc core being *C1ql3*-positive (Fig. S5G, S5H). Given the size and subdivisions of the ventral striatum, it is possible that more specific targeting would yield a higher percentage. Additionally, although possibly unrelated

to the cKO fear memory phenotype, we consistently observed projections of *C1ql3*-positive neurons to the mPFC from the piriform cortex (Fig. 5C, 5F). We conclude that a majority of neurons projecting from the BLA to the ILC and PLC express *C1ql3*, and that at least a fraction of BLA neurons projecting to the NAc do as well.

C1ql3-positive projections to the mPFC likely contribute to fear memory behavior

To investigate whether the neurons expressing *C1ql3* that project to the mPFC contribute to fear memory behavior, we attempted to retrogradely selectively ablate *C1ql3* expression only in BLA neurons that project to the mPFC. For this purpose, we generated AAVs that express wheat germ agglutinin (WGA) fused to Cre (WGA-Cre-IRES-tdTomato). By a poorly understood mechanism, the secreted WGA is taken up by neurons and transported both anterogradely and retrogradely to the nucleus, but is not transferred beyond second order neurons (Gerfen et al., 1982; Ohmoto et al., 2008; Xu and Sudhof, 2013). For use in control mice, we also produced AAV with a mutated Cre (WGA-ΔCre-IRES-tdTomato). In addition to being innervated by *C1ql3*-positive axons, the mPFC also has a small number of *C1ql3*-expressing cells (Fig. 2C, 2D). Since the WGA-Cre AAV will likely also delete *C1ql3* in the injected location in addition to the Cre trans-neuronal transport, we also produced AAV to target Cre locally only at the injection location (Cre-IRES-tdTomato). This allowed us to distinguish between the local effects of *C1ql3* deletion in the mPFC and the effects of *C1ql3* deletion from both the mPFC and neurons innervating the mPFC.

The three AAVs were injected into the mPFC of adult cKO mice (Fig. 6A, 6B). We did not observe an obvious reduction in the number of *C1ql3*-positive somata in the BLA after WGA-Cre expression in the mPFC, consistent with our retrograde rabies virus tracing experiments which suggested that a relatively small fraction of the total *C1ql3*-positive BLA neurons project to the mPFC (Fig. 5). Five weeks post-surgery, mice were tested behaviorally. We found that neither local Cre nor WGA-Cre expression significantly affected open field or elevated plus maze behaviors (Fig. 6C, 6D). In fear memory tests, WGA-Cre expression but not local Cre expression caused a reduction in both contextual and cued fear memory (Fig. 6E). We observed this result despite the relative low efficiency of this this WGA-Cre tool, which was estimated to be <50% (Xu and Sudhof, 2013); apparently, even a partial disruption of the *C1ql3*-dependent fear memory circuit causes a noticeable behavioral deficit. The reductions were not observed after Cre expression only in the mPFC, suggesting that *C1ql3*-positive afferent connections are specifically contributing to the fear memory behaviors. The reduction in cued memory in this experiment further supports the notion that *C1ql3* contributes to both contextual and cued memory. It is also consistent with a model of *C1ql3*-expressing neurons in the BLA projecting to the mPFC and contributing to fear memory behaviors.

It is possible that the *C1ql3*-positive neurons in the BLA project simultaneously to multiple locations. If true, then WGA-Cre expressed in the mPFC and retrogradely transported to the BLA will cause a removal of C1ql3 protein at multiple projection targets, and not solely the mPFC. To address this concern, we simultaneously injected retrograde tracers with different labels into two brain regions. Cholera toxin subunit B (CTB) conjugated to Alexa Fluor 647 was stereotactically injected into the mPFC, while CTB-555 was injected into other known

target areas of BLA projections, including the lateral shell of the N. accumbens, the lacunosum moleculare layer of the ventral hippocampus, and a region containing insular cortex and claustrum (Fig. S6A). As expected, we observed *C1ql3*-positive neurons projecting to the mPFC, as well as to the N. accumbens and insula/claustrum. Relatively few BLA neurons, however, projected to the ventral hippocampus; none of these neurons were located in the anterior BLA where *C1ql3* expression was greatest.

The *C1ql3*-positive mPFC-projecting neurons were examined for co-expression of CTB-555 to quantify the percent of *C1ql3*-postitive BLA neurons that project to both the mPFC and to other locations. We found that ~23% and ~20% of *C1ql3*-postitive mPFC-projecting neurons additionally projected to the N. accumbens and insula/claustrum, respectively (Fig. S6C–H, S6L). In the complementary quantification, we found that ~10% and ~5% of the *C1ql3*-positive projection neurons to the N. accumbens and insula/claustrum, respectively, projected to the mPFC. Almost no BLA neurons that projected to both the mPFC and the ventral hippocampus were detected (Fig. S6I–L). These results show that *C1ql3*-positive mPFC-projection neurons are largely specific for the mPFC; thus, WGA-Cre expression in the mPFC can be expected to primarily cause a removal of C1ql3 protein from mPFC projections. In total, this combined circuit/behavioral analysis suggests that *C1ql3*-expressing neurons in the BLA project to the mPFC and contribute to fear memory.

C1ql3 promotes excitatory synapse density *in vivo*

We next asked whether *C1ql3* expression in the BLA is important for the synaptic projections formed by BLA neurons. Prior anterograde tracing studies showed that the synaptic projections from the BLA to the mPFC localize to cortical layers 1 and 2 of the mPFC (Bacon et al., 1996), suggesting that the *C1ql3* KO may affect synapses in this area. To address this question, we first quantified both excitatory and inhibitory synapse density in the mPFC of constitutive *C1ql3* KO and wild-type adult mice by immunofluorescence labeling for VGluT1 and VGAT, respectively. For quantification, we focused on the outer part of layer 2 and the inner half of layer 1 in the prelimbic cortex (Fig. 7A). We found that *C1ql3* KO mPFC had a significant partial reduction in excitatory synapse density, whereas inhibitory synapse density was unchanged (Fig. 7B, 7C). This decrease in synapse density occurred despite the fact that our retrograde tracing experiments showed that the majority of innervation to the mPFC is from thalamic and ventral hippocampal regions, neither of which express *C1ql3*.

We next tested the role of *C1ql3* in mPFC synapses that specifically originate from the BLA, as opposed to the thalamus, ventral hippocampus, *etc*. We produced AAV vectors that were designed to allow quantification of the number of presynaptic projections of a neuron after the conditional deletion of a gene in that neuron. Two AAVs were constructed, a test AAV (Cre-IRES-tdTomato-SYB2) co-expressing Cre with a tdTomato-synaptobrevin 2 (SYB2) fusion protein, and a control AAV (ΔCre-IRES-tdTomato-SYB2) co-expressing mutant Cre with the same tdTomato-SYB2. These are variants of the SynaptoTag vectors we developed earlier (Xu and Sudhof, 2013). The AAVs were targeted to the BLA of 9-week old *C1ql3* cKO mice with stereotaxic injections (Fig. 7D, 7E). After 5 weeks of expression, we

examined the anterograde distribution and density of tdTomato-positive synaptic puncta terminating in the mPFC.

Consistent with the prior anterograde tracing study (Bacon et al., 1996), the ΔCre-IRES-tdTomato-SYB2 AAV produced a narrow ~100 μm band of synaptic puncta in the prelimbic cortex centered on the boundary of layers 1 and 2, and in layers 2 and 5 of the infralimbic cortex (Fig. 7F left). When the Cre-IRES-tdTomato-SYB2 AAV was used, there was a near total absence of BLA-derived synapses in these same locations (Fig. 7F right), demonstrating that *C1ql3* is required for synapse maintenance in the BLA to mPFC projection. We additionally quantified the projection from the BLA to the N. accumbens shell, where dense tdTomato signal was observed. We also observed a dramatic reduction in presynaptic terminals in the N. accumbens when *C1ql3* was ablated from the BLA projection neurons (Fig. S7A–C), indicating that *C1ql3* is important for the synaptic connections of multiple projections from the BLA.

To test whether *C1ql3* is required for all BLA-derived synaptic projections, we examined the well-established BLA projection to the ventral hippocampus (Janak and Tye, 2015). We observed no mVenus-positive axons in the CA1 region of the ventral hippocampus, suggesting that these projections do not express *C1ql3*. We observed that SynaptoTag expression in the amygdala produced relatively few tdTomato-positive synaptic punctae in the lacunosum moleculare layer of the ventral hippocampus compared to the mPFC or N. accumbens (Fig. S7D–F). This is likely because BLA to hippocampus projections seem to emanate from the posterior BLA, and our SynaptoTag injections targeted the anterior BLA where *C1ql3* expression is more abundant. Regardless, we detected no reduction in presynaptic terminal density of BLA projections to the hippocampus when *C1ql3* was ablated from the BLA, suggesting that the reduction of synapse density in the mPFC and N. accumbens is unlikely to be caused by toxicity of the Cre-IRES-tdTomato-SYB2 AAV.

Finally, to confirm the reduction in excitatory synapses observed in the *C1ql3* KO mPFC and to explore the possibility that the structure of synapses may be changed by *C1ql3*, we performed transmission electron microscopy on mPFC sections from KO and wild-type adult mice. Guided by the band of presynaptic tdTomato-SYB2 observed in Fig. 7F after SynaptoTag tracing, we focused on the narrow boundary between layers 1 and 2 of the prelimbic cortex, where the fraction of innervation from the BLA was likely greatest. Quantification of asymmetric (excitatory) synapse density revealed a significant reduction in *C1ql3* KO mice compared to littermate wild-type mice (Fig. 8A, 8C). We also quantified the density of perforated synapses, which often correlate with increased synaptic activity (Neuhoff et al., 1999). Not surprisingly given the reduced density of total asymmetric synapses, we found a reduced density of perforated synapses (Fig. 8B, 8D left). When perforated synapses were graphed as a fraction of the total synapses, we noted a trend for a reduced fraction of synapses that were perforated (Fig. 8D right). In contrast, we found no change in synapse structure, as analyzed via the postsynaptic density (PSD) length, PSD width, synaptic cleft width, presynaptic terminal area, terminal perimeter, number of vesicles per terminal, number of docked vesicles per terminal, vesicle density, or vesicle diameter (Fig. 8E–M). Combining the *in vivo* and *in vitro* results using multiple experimental techniques, we conclude that C1ql3 promotes both excitatory synaptogenesis and synapse

maintenance. Furthermore, the reduction of synapses in the mPFC areas targeted by *C1ql3*-positive BLA neurons suggests that the fear memory phenotype in the *C1ql3* KO and cKO mice is due to this loss of synapses.

DISCUSSION

In brain, synapses are formed and continuously restructured throughout life with an amazing specificity and activity-dependent plasticity based on our different experiences. How synapses are organized so precisely remains largely unknown. In the present study, we explored the potential role of C1ql proteins as synaptic organizers that contribute to the formation and/or function of a selected set of synapses. *A priori*, C1ql proteins are ideally suited for such a role because of their similarity to cerebellins, which are known synaptic organizer molecules (Matsuda et al., 2010; Uemura et al., 2010).

We made five principal observations. First, we showed in cultured neurons that *C1ql* expression is regulated by neuronal activity, that a general knockdown of C1ql's leads to a loss of synapses, and that the *C1ql* knockdown also abolishes the increase in synapse numbers induced by prolonged silencing of neurons (Fig. 1, S1). Second, focusing on C1ql3 for *in vivo* studies because it is the most widely expressed C1ql isoform, we generated knockin mice that allow conditional KO of *C1ql3* and also enable identification of *C1ql3*-expressing cells via co-expressed mVenus. Using this knockin allele, we demonstrated that *C1ql3* is expressed throughout brain in a subset of neurons present in selected brain areas, including the amygdala, dentate gyrus, and insular/perirhinal/piriform/retrosplenial cortices (Fig. 2, S2). The restricted expression of C1ql3 suggests a discrete role specific to particular circuits, neurons, and synapses. Third, we showed that constitutive *C1ql3* KO mice exhibit diverse but selective behavioral abnormalities, several of which are broadly related to emotionally salient memories, including impairments in fear memories, cocaine-conditioned place preference, and lithium-conditioned place aversion (Fig. 3). Fourth, we demonstrated that selective ablation of *C1ql3* in the amygdala impairs fear memories but not cocaine-conditioned place preference, and that *C1ql3*-expressing amygdala neurons project in part to the mPFC, a brain region which is essential for such memories (Fig. 4, S4, 5, S5, and S6). Furthermore, ablation of *C1ql3* from neurons that project to the mPFC also caused fear memory deficits (Fig. 6). Fifth and finally, we showed that constitutive deletion of *C1ql3* reduces the excitatory synapse density in the mPFC, and that conditional deletion of *C1ql3* from the BLA causes a loss of nearly all of the BLA output synapses in the mPFC and the N. accumbens (Fig. 7, 8, S7). Viewed together, these results support the notion that C1ql3 is specifically required for excitatory synapse formation and/or maintenance in a small subset of central neurons that are characterized by contributions to emotionally salient memories, such as fear conditioning memory.

C1ql3 is essential for normal emotional memory

The common impairments of cocaine-conditioned place preference, lithium-conditioned place aversion, and fear conditioning behavior caused by the *C1ql3* KO (Fig. 3G–3M) lead us to propose that *C1ql3* is required for a subset of memories that involve classical conditioning and motivationally significant or emotionally salient stimuli. It is possible that

the apparent reduction in anxiety-like state we observed in the elevated plus maze (Fig. 3F) is also related to this memory phenotype. The memory deficit appears to involve immediate fear memories, as the phenotype was clear in the 1 min post-training period in the fear conditioning experiments (Fig. 3H). These results are not due to a hippocampal-dependent deficit in the mutants' ability to remember the context of the conditioning chambers *per se* because *C1ql3* KO mice performed normally in the Morris water maze, Y-maze, and novel object recognition task (Fig. 3N–3P). Possibly such assays are not sufficiently emotionally arousing to render them dependent on *C1ql3*.

Our Cre-virus manipulations in cKO mice revealed that the reduced fear memory phenotype in *C1ql3* KO mice could be traced specifically to *C1ql3* expression in a subset of BLA neurons (Fig. 4). Targeting the BLA for Cre-mediated recombination caused *C1ql3* cKO mice to exhibit contextual fear memory deficits similar to those of constitutive KO mice. Moreover, a test for cued fear memory 4 weeks post-training revealed that *C1ql3* also has a role in cued memory, at least in the cKO mice. It is unclear why the contextual memory deficits are apparent immediately after training while the cued memory deficits appeared only weeks later. Perhaps cued fear memory may be more robust than contextual fear memory in our experimental paradigm, and thus more difficult to perturb. The conditional mutants had no deficit in any other assay used, indicating that the other phenotypes observed in constitutive KO mice do not require *C1ql3* expression in the BLA. It remains to be determined which other brain structures might be involved in the role of *C1ql3* in these behaviors.

Our circuit analysis of *C1ql3*-expressing BLA neurons began with the clue from the literature that *C1ql3* is a marker for *Thy1-YFP-H* neurons in the amygdala (Sugino et al., 2006). Indeed, the YFP expression pattern in the amygdala is remarkably similar to our *C1ql3*/mVenus expression. Mapping of YFP expression suggested that these BLA neurons project to the mPFC (Porrero et al., 2010), which we have confirmed here (Fig. S5). The mPFC projection was particularly interesting because elegant tracing studies showed that intermingled but distinct subsets of neurons have unique projection targets. For example, 'fear neurons' project from the BLA to the prelimbic cortex and are active during fear training, while 'extinction neurons' project from the BLA to the infralimbic cortex and are active during fear memory extinction training (Herry et al., 2008; Senn et al., 2014). It was possible that *C1ql3* would be a specific marker for one of these subsets of neurons. However, we found that *C1ql3*-expressing BLA neurons send projections to both the prelimbic and infralimbic cortex (Fig. 5, S5). Nonetheless, a role for C1ql3 at synapses in the mPFC is consistent with our finding that the *C1ql3* KO impairs fear memories, and it is likely that the reduced excitatory synapse density in the mPFC areas targeted by BLA projection neurons is causative in the fear memory phenotype. Given *C1ql3's* expression in a small but diverse subset of brain regions, it is likely that a similar reduction in excitatory synapses in distinct circuits would explain the other observed behavior deficits in the constitutive KO mice (*e.g.,* conditioned place preference).

C1ql3 controls synapse density

Recent papers investigating the cerebellum concluded that presynaptically secreted C1ql1 from the inferior olive climbing fibers interacts with postsynaptic BAI3 on Purkinje cells, and that this interaction promotes synapse maturation (Kakegawa et al., 2015; Sigoillot et al., 2015). Whether the mechanism of C1ql's influence on synapses is similar across family members remains to be determined, although C1ql1 and C1ql3 have similar affinities for BAI3 (Bolliger et al., 2011). In our work, we present evidence that *C1ql* genes promote and/or maintain excitatory synapse density both in cultured neurons and in the mPFC and N. accumbens (Fig. 1, 7, 8, S7). The reductions in excitatory synapses are consistent both with *C1ql3*'s specific expression in excitatory cortical/BLA neurons and with BAI3's postsynaptic localization at excitatory synapses. Additionally, *C1ql* expression is up-regulated after neuronal activity blockade in cultured neurons (Fig. 1C), consistent with a role for C1ql3 in synapse density. Viewed together, these data suggest that *C1ql3* is essential for synapse maintenance, and may additionally via the same molecular activity that mediates synapse maintenance contribute to synaptic formation.

These observations suggest at least two possible explanations for how C1ql3 influences synapses that are not necessarily mutually exclusive (Fig. 8N). First, C1ql3 is transported along axons, secreted, binds to BAI3, and initiates an intracellular signaling cascade. It is likely that axonal transport and secretion is a general property of all gC1q domain-containing family members, as cerebellin-1 and C1ql1 both have this property (Kakegawa et al., 2015; Wei et al., 2009). The second possible explanation for how C1ql3 influences synapses is that a yet to be identified membrane-tethered binding partner of C1ql3 presents the complex on the presynaptic membrane surface (Fig. 8N). This complex might then bind to the postsynaptic receptor, creating a trans-synaptic ternary adhesion complex comparable to the neurexin/cerebellin-1/GluRδ2 complex (Matsuda and Yuzaki, 2011; Uemura et al., 2010). The function of a C1ql3-based trans-synaptic cell-adhesion complex could be structural, could act to localize pre- and postsynaptic binding partners to proper locations, or may mediate signaling. In any case, a possible functional consequence of the C1ql3-BAI3 interaction could be modulation of the dendritic actin cytoskeleton. F-actin is enriched in spines, provides structural integrity, and organizes required proteins to the postsynaptic density (Lin and Koleske, 2010) and the BAI1 paralog has already been shown to be postsynaptically localized and to regulate the dendritic actin cytoskeleton (Duman et al., 2013; Stephenson et al., 2013).

Many questions remain. What are the behavioral consequences of ablating *C1ql3* from the other brain structures where it is expressed? What is the precise biochemical mechanism by which C1ql3 protein initiates and/or stabilizes the synapse? And does this mechanism involve a potential presynaptic binding partner or C1ql3-initiated GPCR signaling through BAI3? Is there any cross-talk between the C1ql pathway and those of homologs like the cerebellins and C1q's? Why do some synaptic projections appear to require C1ql's, but others seem to be independent of these genes? Answers to these questions will likely yield greater insights into the molecular logic of how synaptic proteins orchestrate synapse formation, modification, and function, and to ultimately provide an explanation for how these events influence behaviors.

METHODS

Neuronal culture experiments

All neurons were cultured from newborn mice as described (Bolliger et al., 2011). Hippocampal cultures were made from CD-1 mice. For lentivirus experiments, cultured neurons were infected on DIV5. For *in vitro* experiments with AAV, 0.1 μl (titer = 10^{10}/ml) of purified AAV was added to cultured neurons on DIV8. Analysis on cultures was performed at DIV14. For figure 1C, drugs were applied at DIV14 and RNA harvested 3 days later. For quantification of synaptic puncta, a novel program was coded for Mathmatica (Wolfram) to quantify puncta density, surface area, and mean fluorescence intensity. Secondary dendrites on pyramidal-shaped neurons were photographed for quantification. Refer to supplemental online material for additional details.

C1ql3 cKO allele

The targeting vector was constructed using the recombineering technique as described in (Liu et al., 2003) and was electroporated into ES cells derived from F1 hybrid blastocyst of 129S6 x C57BL/6J. Chimeric mice were generated by aggregating ES cells with 8-cell embryos of CD-1 strain. The correct targeting was further confirmed by homozygosity testing. Mice harboring the novel allele were back-crossed to the C57BL6/J strain ($C1ql3^{tm1.1Sud}$ RRID: MGI_5779515).

Behavior

All behavior experiments were performed on littermate male mice. $C1ql3^{+/+}$, $C1ql3^{+/-}$, and $C1ql3^{-/-}$ ($C1ql3^{tm1.2Sud}$ RRID: MGI_5779517) mice were obtained by breeding $C1ql3^{+/-}$ mice. For the germline mutant analysis all mice were 2–3 months old. For virus injected mice, 3–5 months old.

Fear conditioning—2 min measurement of baseline activity in training chamber (mice were not pre-exposed to the chamber) followed by 5 training cycles each lasting 47 s and consisting of 15 s tone (90 dB volume) and 2 s foot shock (0.26 mA average intensity) co-terminating with the tone, 32 s inter-cycle interval. After last shock, 1 additional minute in chamber. 1 day later mouse placed in training chamber and observed for 2 min. 2 days later mouse placed in an altered context chamber with vanilla scent and observed for 2 min to measure new baseline activity, followed by 1 min tone.

All mouse work was approved by animal use committees at Stanford University.

Viruses

The following adeno-associated viruses (AAV-DJ) were used in this study, all with a synapsin promoter: ΔCre-P2A-mCherry, Cre-IRES-C1ql3-HA, Cre only, ΔCre-IRES-tdTomato-SYB2, Cre-IRES-tdTomato-SYB2, WGA-ΔCre-IRES-tdTomato, WGA-Cre-IRES-tdTomato, and Cre-IRES-tdTomato. For the control vector (*i.e.* ΔCre), the Cre sequence was half-truncated creating a non-functional enzyme. For *C1ql* RNAi and rescue, the following lentiviruses were used: pL309 +shRNA#65, empty pL309 for control, pL309 +mCherry-IRES-C1ql3-HA, pL309 +shRNA#65 +mCherry-IRES-C1ql3-HA. shRNA

designed to target *C1ql1–3*. Rabies-tdTomato was generous gift from Robert Malenka's lab (Lim et al., 2012).

Stereotaxic virus infection

All surgeries performed on littermate male mice 9 weeks old and 0.2 – 0.5 μl (titer = 10^{10}/ml) purified AAV injected per location. All experiments began 4 or 5 weeks after surgery.

Supplementary Material

Refer to Web version on PubMed Central for supplementary material.

Acknowledgments

We thank Sameer Arya for programming the Mathematica application for synapse quantification and Lulu Chen for designing the *C1ql* shRNA sequence. We are grateful to Lu Chen, Rob Malenka, Patrick Rothwell, Elizabeth Steinberg, and Sarah Ruediger for helpful discussions. This work was supported by grants from the NIH (MH052804 and MH086403 to TCS), by fellowships from NIDA (F32 DA031654 to DCM) and the Max-Planck Society (to SR).

References

Arendt KL, Sarti F, Chen L. Chronic inactivation of a neural circuit enhances LTP by inducing silent synapse formation. J Neurosci. 2013; 33:2087–2096. [PubMed: 23365245]

Bacon SJ, Headlam AJ, Gabbott PL, Smith AD. Amygdala input to medial prefrontal cortex (mPFC) in the rat: a light and electron microscope study. Brain research. 1996; 720:211–219. [PubMed: 8782914]

Bardo MT, Bevins RA. Conditioned place preference: what does it add to our preclinical understanding of drug reward? Psychopharmacology. 2000; 153:31–43. [PubMed: 11255927]

Bolliger MF, Martinelli DC, Sudhof TC. The cell-adhesion G protein-coupled receptor BAI3 is a high-affinity receptor for C1q-like proteins. Proc Natl Acad Sci U S A. 2011; 108:2534–2539. [PubMed: 21262840]

Caselli C. Role of adiponectin system in insulin resistance. Molecular genetics and metabolism. 2014

DeRosse P, Lencz T, Burdick KE, Siris SG, Kane JM, Malhotra AK. The genetics of symptom-based phenotypes: toward a molecular classification of schizophrenia. Schizophr Bull. 2008; 34:1047–1053. [PubMed: 18628273]

Duman JG, Tzeng CP, Tu YK, Munjal T, Schwechter B, Ho TS, Tolias KF. The adhesion-GPCR BAI1 regulates synaptogenesis by controlling the recruitment of the Par3/Tiam1 polarity complex to synaptic sites. J Neurosci. 2013; 33:6964–6978. [PubMed: 23595754]

Duvarci S, Pare D. Amygdala microcircuits controlling learned fear. Neuron. 2014; 82:966–980. [PubMed: 24908482]

Feng G, Mellor RH, Bernstein M, Keller-Peck C, Nguyen QT, Wallace M, Nerbonne JM, Lichtman JW, Sanes JR. Imaging neuronal subsets in transgenic mice expressing multiple spectral variants of GFP. Neuron. 2000; 28:41–51. [PubMed: 11086982]

Gerfen CR, O'Leary DD, Cowan WM. A note on the transneuronal transport of wheat germ agglutinin-conjugated horseradish peroxidase in the avian and rodent visual systems. Experimental brain research. 1982; 48:443–448. [PubMed: 6185358]

Ghai R, Waters P, Roumenina LT, Gadjeva M, Kojouharova MS, Reid KB, Sim RB, Kishore U. C1q and its growing family. Immunobiology. 2007; 212:253–266. [PubMed: 17544811]

Hamann J, Aust G, Arac D, Engel FB, Formstone C, Fredriksson R, Hall RA, Harty BL, Kirchhoff C, Knapp B, et al. International Union of Basic and Clinical Pharmacology. XCIV. Adhesion G protein-coupled receptors. Pharmacological reviews. 2015; 67:338–367. [PubMed: 25713288]

Herry C, Ciocchi S, Senn V, Demmou L, Muller C, Luthi A. Switching on and off fear by distinct neuronal circuits. Nature. 2008; 454:600–606. [PubMed: 18615015]

Hirai H, Pang Z, Bao D, Miyazaki T, Li L, Miura E, Parris J, Rong Y, Watanabe M, Yuzaki M, et al. Cbln1 is essential for synaptic integrity and plasticity in the cerebellum. Nat Neurosci. 2005; 8:1534–1541. [PubMed: 16234806]

Iijima T, Miura E, Watanabe M, Yuzaki M. Distinct expression of C1q-like family mRNAs in mouse brain and biochemical characterization of their encoded proteins. Eur J Neurosci. 2010; 31:1606–1615. [PubMed: 20525073]

Janak PH, Tye KM. From circuits to behaviour in the amygdala. Nature. 2015; 517:284–292. [PubMed: 25592533]

Kakegawa W, Mitakidis N, Miura E, Abe M, Matsuda K, Takeo YH, Kohda K, Motohashi J, Takahashi A, Nagao S, et al. Anterograde C1ql1 signaling is required in order to determine and maintain a single-winner climbing fiber in the mouse cerebellum. Neuron. 2015; 85:316–329. [PubMed: 25611509]

Lanoue V, Usardi A, Sigoillot SM, Talleur M, Iyer K, Mariani J, Isope P, Vodjdani G, Heintz N, Selimi F. The adhesion-GPCR BAI3, a gene linked to psychiatric disorders, regulates dendrite morphogenesis in neurons. Mol Psychiatry. 2013; 18:943–950. [PubMed: 23628982]

Lim BK, Huang KW, Grueter BA, Rothwell PE, Malenka RC. Anhedonia requires MC4R-mediated synaptic adaptations in nucleus accumbens. Nature. 2012; 487:183–189. [PubMed: 22785313]

Lin YC, Koleske AJ. Mechanisms of synapse and dendrite maintenance and their disruption in psychiatric and neurodegenerative disorders. Annual review of neuroscience. 2010; 33:349–378.

Liu P, Jenkins NA, Copeland NG. A highly efficient recombineering-based method for generating conditional knockout mutations. Genome research. 2003; 13:476–484. [PubMed: 12618378]

Liu QR, Drgon T, Johnson C, Walther D, Hess J, Uhl GR. Addiction molecular genetics: 639,401 SNP whole genome association identifies many “cell adhesion” genes. American journal of medical genetics Part B, Neuropsychiatric genetics : the official publication of the International Society of Psychiatric Genetics. 2006; 141B:918–925.

Matsuda K, Miura E, Miyazaki T, Kakegawa W, Emi K, Narumi S, Fukazawa Y, Ito-Ishida A, Kondo T, Shigemoto R, et al. Cbln1 is a ligand for an orphan glutamate receptor delta2, a bidirectional synapse organizer. Science. 2010; 328:363–368. [PubMed: 20395510]

Matsuda K, Yuzaki M. Cbln family proteins promote synapse formation by regulating distinct neurexin signaling pathways in various brain regions. Eur J Neurosci. 2011; 33:1447–1461. [PubMed: 21410790]

Naqvi NH, Bechara A. The insula and drug addiction: an interoceptive view of pleasure, urges, and decision-making. Brain structure & function. 2010; 214:435–450. [PubMed: 20512364]

Neuhoff H, Roeper J, Schweizer M. Activity-dependent formation of perforated synapses in cultured hippocampal neurons. Eur J Neurosci. 1999; 11:4241–4250. [PubMed: 10594650]

Ohmoto M, Matsumoto I, Yasuoka A, Yoshihara Y, Abe K. Genetic tracing of the gustatory and trigeminal neural pathways originating from T1R3-expressing taste receptor cells and solitary chemoreceptor cells. Molecular and cellular neurosciences. 2008; 38:505–517. [PubMed: 18539481]

Porrero C, Rubio-Garrido P, Avendano C, Clasca F. Mapping of fluorescent protein-expressing neurons and axon pathways in adult and developing Thy1-eYFP-H transgenic mice. Brain research. 2010; 1345:59–72. [PubMed: 20510892]

Ressl S, Vu BK, Vivona S, Martinelli DC, Sudhof TC, Brunger AT. Structures of C1q-like proteins reveal unique features among the C1q/TNF superfamily. Structure. 2015; 23:688–699. [PubMed: 25752542]

Senn V, Wolff SB, Herry C, Grenier F, Ehrlich I, Grundemann J, Fadok JP, Muller C, Letzkus JJ, Luthi A. Long-range connectivity defines behavioral specificity of amygdala neurons. Neuron. 2014; 81:428–437. [PubMed: 24462103]

Sigoillot SM, Iyer K, Binda F, Gonzalez-Calvo I, Talleur M, Vodjdani G, Isope P, Selimi F. The Secreted Protein C1QL1 and Its Receptor BAI3 Control the Synaptic Connectivity of Excitatory Inputs Converging on Cerebellar Purkinje Cells. Cell reports. 2015

Stephenson JR, Paavola KJ, Schaefer SA, Kaur B, Van Meir EG, Hall RA. Brain-Specific Angiogenesis Inhibitor-1 Signaling, Regulation and Enrichment in the Postsynaptic Density. J Biol Chem. 2013

Stevens B, Allen NJ, Vazquez LE, Howell GR, Christopherson KS, Nouri N, Micheva KD, Mehalow AK, Huberman AD, Stafford B, et al. The classical complement cascade mediates CNS synapse elimination. Cell. 2007; 131:1164–1178. [PubMed: 18083105]

Sugino K, Hempel CM, Miller MN, Hattox AM, Shapiro P, Wu C, Huang ZJ, Nelson SB. Molecular taxonomy of major neuronal classes in the adult mouse forebrain. Nat Neurosci. 2006; 9:99–107. [PubMed: 16369481]

Uemura T, Lee SJ, Yasumura M, Takeuchi T, Yoshida T, Ra M, Taguchi R, Sakimura K, Mishina M. Trans-synaptic interaction of GluRdelta2 and Neurexin through Cbln1 mediates synapse formation in the cerebellum. Cell. 2010; 141:1068–1079. [PubMed: 20537373]

Wei P, Rong Y, Li L, Bao D, Morgan JI. Characterization of trans-neuronal trafficking of Cbln1. Molecular and cellular neurosciences. 2009; 41:258–273. [PubMed: 19344768]

Xu W, Sudhof TC. A neural circuit for memory specificity and generalization. Science. 2013; 339:1290–1295. [PubMed: 23493706]

Highlights

- C1ql3 is expressed in discrete brain structures and subsets of excitatory neurons
- C1ql3 promotes excitatory synapse formation and maintenance *in vitro* and *in vivo*
- C1ql3 is required for implicit association memories of emotionally salient stimuli
- C1ql3-expressing BLA neurons project to mPFC and contribute to fear memory behavior

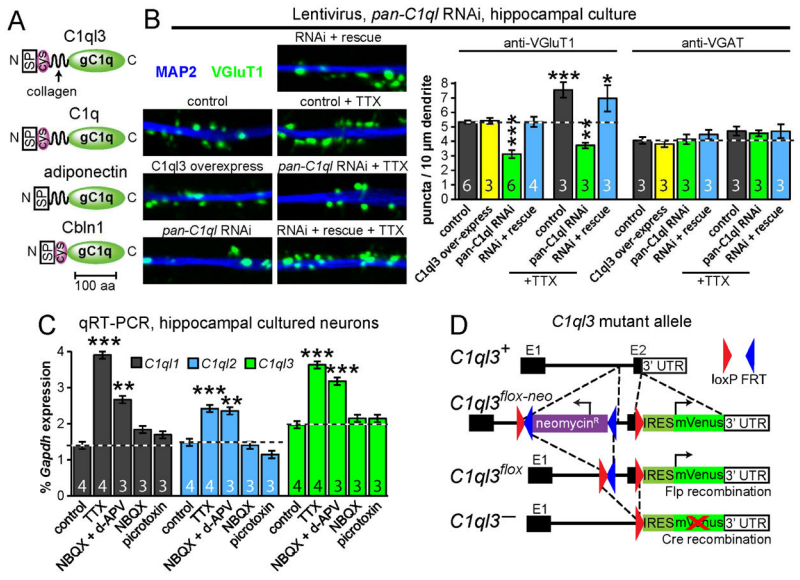

Fig. 1. RNAi-mediated knockdown of *C1ql's* reduces synapse density in cultured neurons and neuronal activity regulates *C1ql* expression

(**A**) Domain structures of gC1q-domain proteins (C1ql3, C1q, adiponectin, and Cbln1; abbreviations: SP, signal peptide; cys, conserved cysteines; gC1q, globular C1q domain).

(**B**) *C1ql* knockdown decreases excitatory synapse density (left, representative images of cultured hippocampal neurons immunostained for VGluT1 and MAP2; right, summary graphs of the density of synaptic puncta). Neurons were infected at DIV5 with control or *C1ql* knockdown lentivirus with or without simultaneous co-expression of C1ql3, and examined at DIV14. Neurons were analyzed with and without a 3-day TTX treatment (from DIV11-DIV14) as indicated.

(**C**) Activity blockade increased *C1ql1–3* expression. Cultured neurons were treated with TTX (1 µM), NBQX (10 µM), d-APV (50 µM), or picrotoxin (50 µM) from DIV14-DIV17, after which total mRNA was harvested and analyzed by qRT-PCR.

(**D**) Targeting scheme for conditional *C1ql3-mVenus* mutant allele.

Data in B and C are means ± SEM. Numbers in bar diagrams indicate number of independent experiments. Statistical comparisons were performed using 1-way ANOVA with Bonferroni's post-hoc test (* $p \leq 0.05$, ** $p \leq 0.01$, *** $p \leq 0.001$). See also Fig. S1.

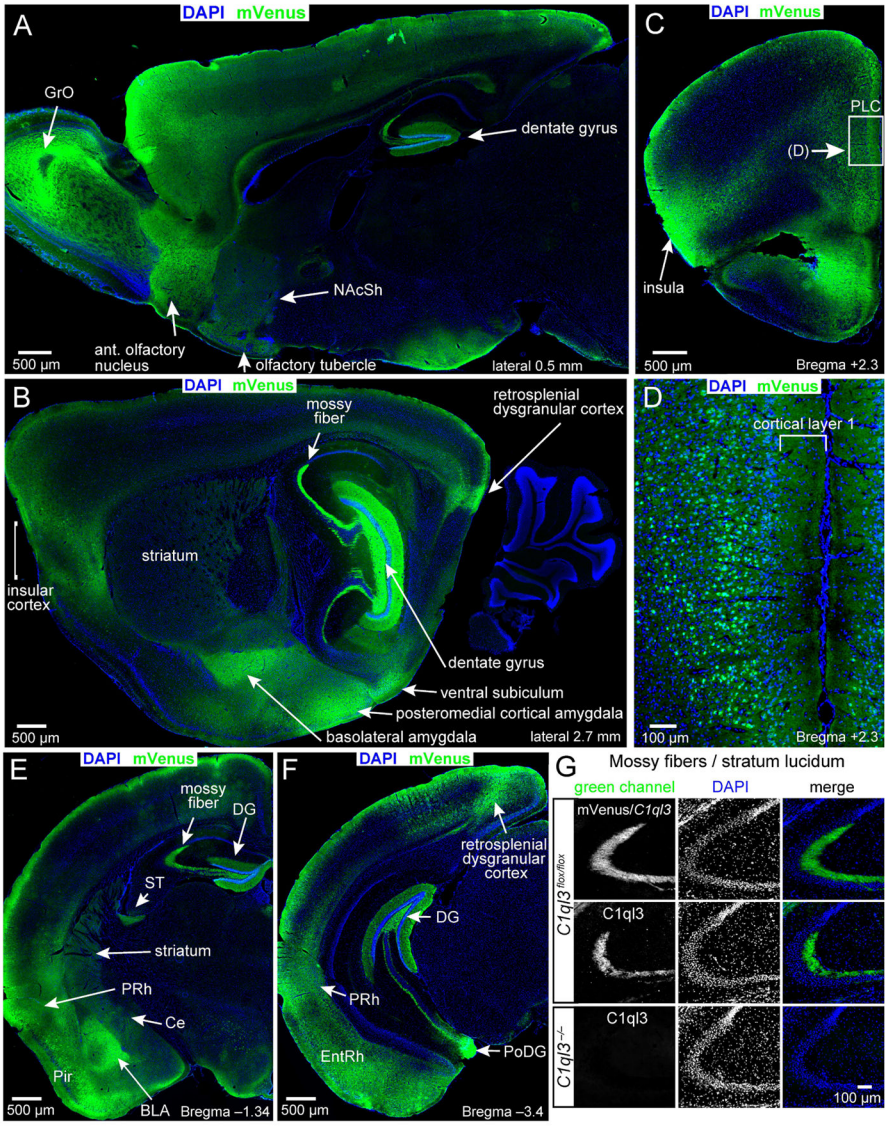

Fig. 2. *C1ql3* is expressed in specific brain structures and discrete subsets of neurons

(**A**–**F**) Immunofluorescence staining of sagittal and coronal sections from adult mice for mVenus in *C1ql3*-expressing cells and labeling with DAPI for cell nuclei (abbreviations: BLA, basolateral amygdala; Ce, central amygdala; DG, dentate gyrus; EntRh, entorhinal cortex; GrO, olfactory bulb granule cell layer; NAcSh, nucleus accumbens shell, Pir, piriform cortex; PoDG, polymorphic DG; PRh, perirhinal cortex; PLC, prelimbic cortex; ST, stria terminalis). Panel D is a magnification of the boxed region in panel C.

(**G**) mVenus (top row) and C1ql3 immunofluorescence staining (bottom 2 rows) of presynaptic mossy-fiber nerve terminals in the stratum lucidum of the CA3 region of the hippocampus. See also Fig. S2.

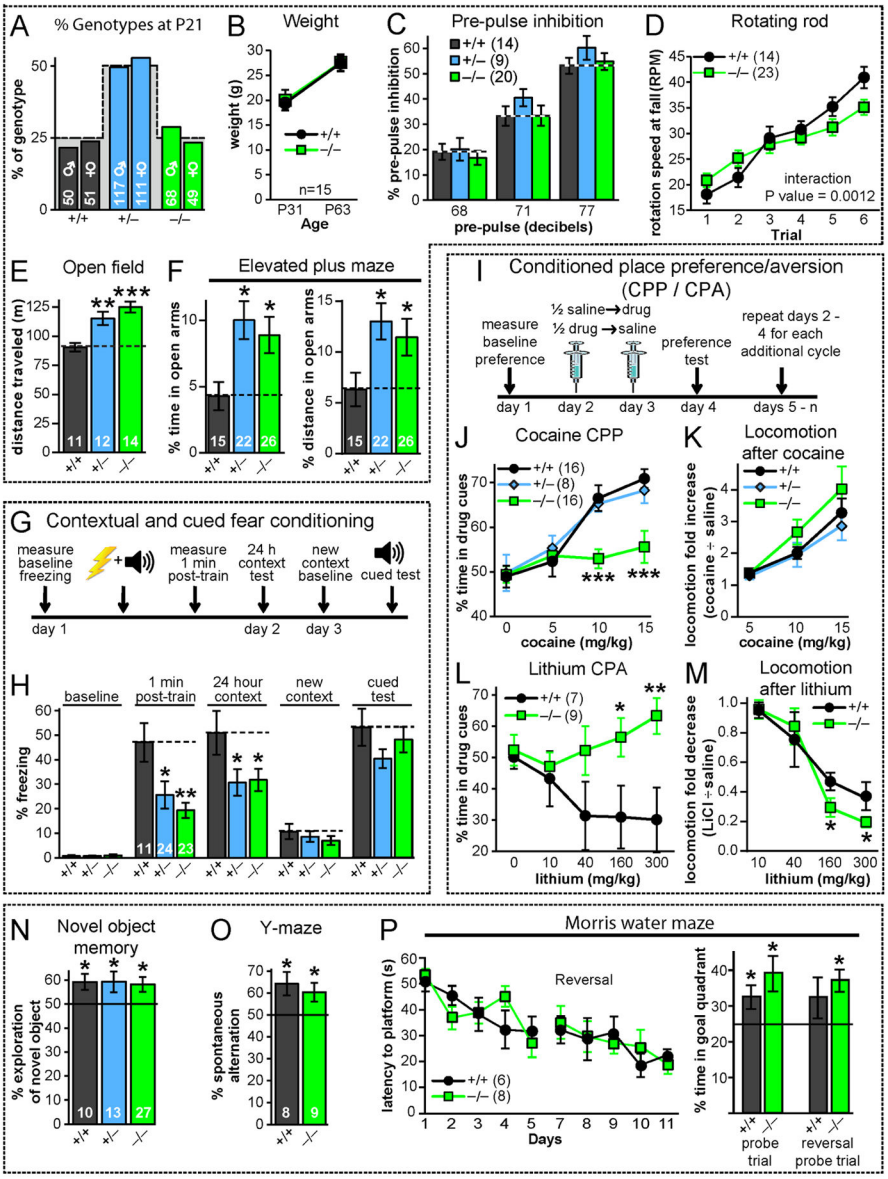

Fig. 3. Constitutive *C1ql3* KO mice exhibit discrete behavioral impairments

(**A**) *C1ql3* KO mice are recovered in the expected Mendelian ratio (dashed line) from offspring of heterozygous parents.

(**B**) Homozygous *C1ql3* KO mice exhibit no decrease in weight at P31 and P63.

(**C**) *C1ql3* KO mice display no phenotype in pre-pulse inhibition of the acoustic startle response (115 decibel startle) at the indicated pre-pulse decibel levels.

(**D**) *C1ql3* KO mice exhibit a modest impairment in motor learning on the accelerating rotating rod (3 trials per day for 2 days).

(**E**) *C1ql3* KO mice are hyperactive in a 20 min open field test.

(**F**) *C1ql3* KO mice display increased time and distance traveled in the open arms of the elevated plus maze.

(**G**) Experimental design for measurements of contextual and cued fear memory.

(**H**) *C1ql3* KO mice exhibit reduced contextual fear memory in the first minute and 24 h after training.
(**I**) Experimental design for conditioned place preference (CPP)/conditioned place aversion (CPA) experiments. Mice explored the chamber for 20 min per session.
(**J**) Homozygous *C1ql3* KO mice display a complete loss of cocaine-induced CPP.
(**K**) *C1ql3* KO mice exhibit no change in cocaine-induced increase in locomotor activity.
(**L**) *C1ql3* KO mice display a complete loss of lithium-induced CPA (distinct cohort from CPP mice).
(**M**) *C1ql3* KO mice exhibit no major change in lithium-induced decrease in locomotor activity.
(**N**) *C1ql3* KO mice display no impairment in novel object recognition (% time exploring a novel object during the first 20 sec measured 24 hours after mice were habituated with 2 identical objects).
(**O**) *C1ql3* KO mice exhibit no change in spontaneous alternating Y-maze performance (consecutive entry into each of the 3 arms in a Y-maze was scored for 5 min).
(**P**) *C1ql3* KO mice exhibit no change in spatial learning in the Morris water maze test (left, latency to reach hidden platform during a 5-day training period and the reversal test with the platform moved to new quadrant; right, % time spent in the goal quadrant during probe trials on days 6 and 12 in which the platform was completely removed).
Data are means ± SEM; the number of mice analyzed is displayed in each graph. Statistical analyses were performed using repeated measures 2-way ANOVA with post-hoc Bonferroni's test (panels D,H,J-M), 1-way ANOVA with post-hoc Bonferroni's test (panels E,F), and univariate t-test against chance, indicated by black line (panels N-P). See also Fig. S3.

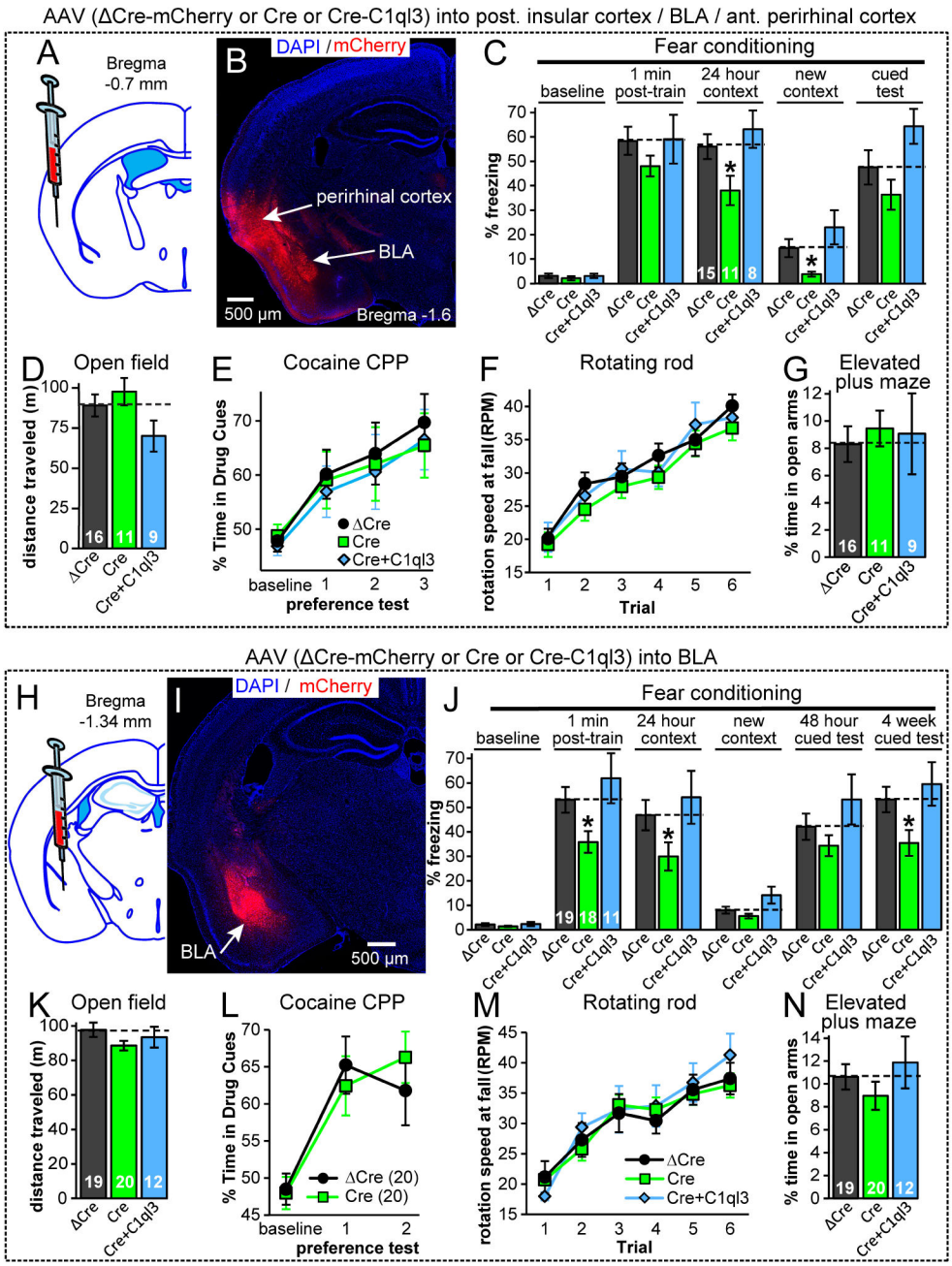

Fig. 4. Conditional KO of *C1ql3* in the BLA impairs fear memories

(**A**) Strategy for region-specific cKO of *C1ql3* in the posterior insula. AAVs encoding Cre, ΔCre-mCherry, or Cre-IRES-C1ql3 were stereotactically injected into 9-week old cKO mice and analyzed 4 weeks later.

(**B**) Representative image of the distribution of mCherry after AAV injection as described in A. Image illustrates the broad distribution of AAV infection in the BLA and the perirhinal cortex in addition to the posterior insula, which is not shown.

(**C**) *C1ql3* cKO mice infected with Cre AAV displayed impaired contextual fear memory.

(**D–G**) *C1ql3* cKO mice infected with Cre AAV displayed no phenotype in the open field test, cocaine-CPP (10 mg/kg cocaine repeated for each conditioning cycle), rotating rod assay, and the elevated plus maze.

(**H–N**) Same as A–G, but for mice in which *C1ql3* was conditionally deleted only in the BLA. In (J), mice were additionally tested for cued memory in the altered context 4 weeks post-training, revealing a memory deficit.

Data are means ± SEM; the number of mice analyzed is displayed in each graph. Statistical analyses were performed using repeated measures 2-way ANOVA with post-hoc Bonferroni's test (C,J). See also Fig. S4.

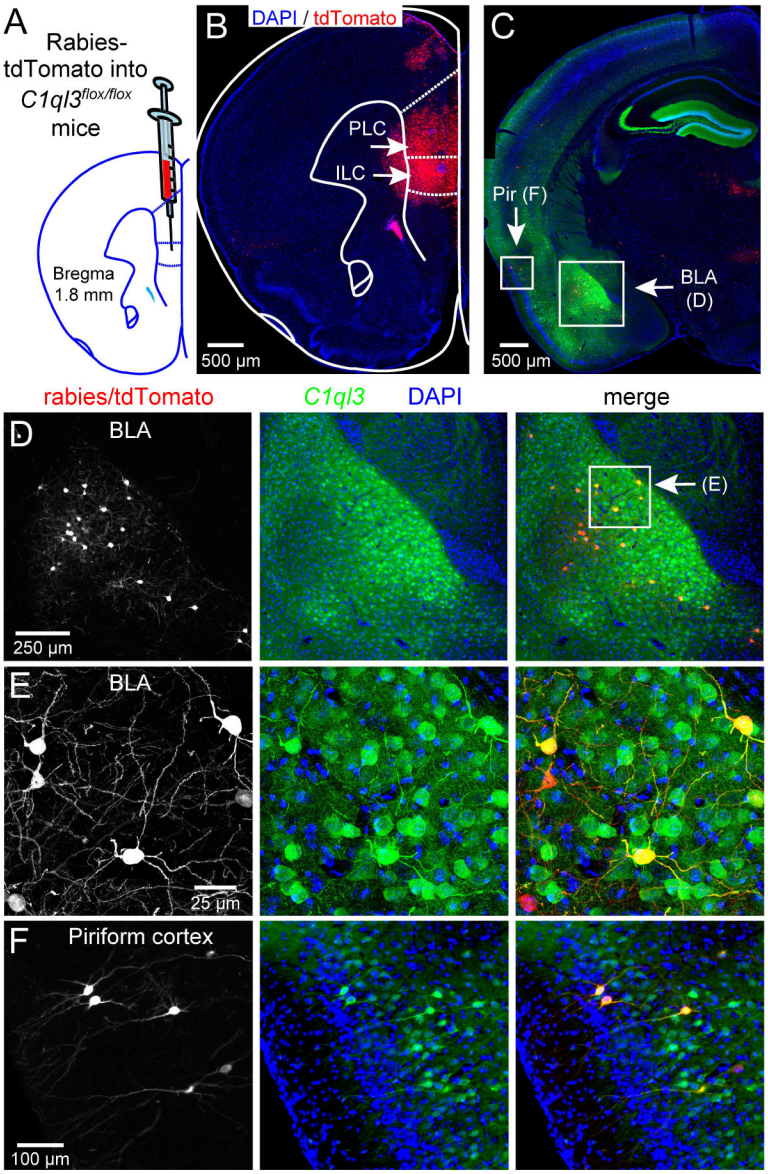

Fig. 5. *C1ql3*-expressing neurons in the BLA project to the mPFC

(**A**) Strategy for stereotactic injections of tdTomato-expressing rabies virus as a retrograde tracer into the mPFC of 9 week old *C1ql3*$^{flox/flox}$ mVenus-reporter mice.

(**B**) Representative section to illustrate tdTomato expression after rabies virus injection (PLC, prelimbic cortex; ILC, infralimbic cortex).

(**C**) Representative section to illustrate tdTomato/*C1ql3* co-expression in the BLA and piriform cortex.

(**D**) Magnification of boxed BLA region in panel C.

(**E**) Magnification of boxed region in panel D.

(**F**) Magnification of boxed piriform region in panel C.

See also Fig. S5.

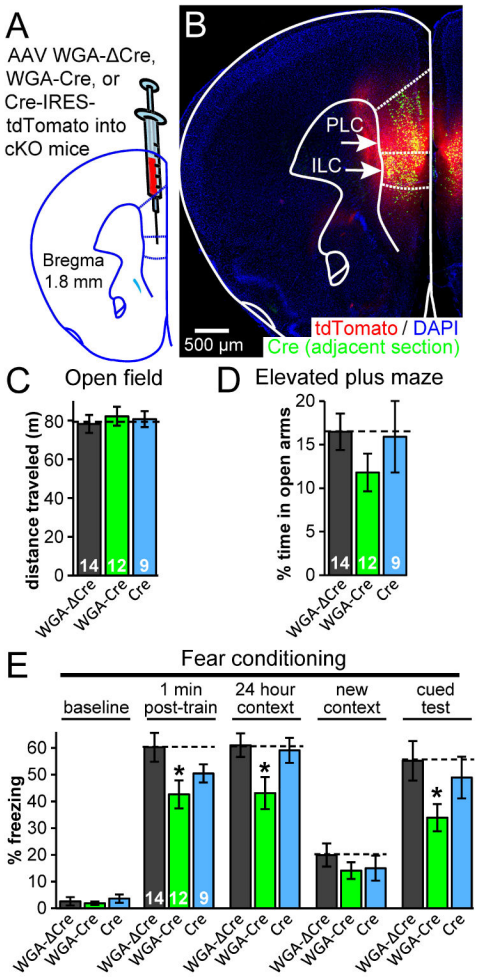

Fig. 6. *C1ql3*-positive projections to the mPFC likely contribute to fear memory

(**A**) Strategy for conditional deletion of *C1ql3* from neurons that project to the mPFC. AAVs encoding WGA-ΔCre-IRES-tdTomato, WGA-Cre-IRES-tdTomato, or Cre-IRES-tdTomato were stereotactically injected into 9 week old mice.

(**B**) Representative section to illustrate tdTomato and Cre expression after AAV injection. Immunofluorescence for the flag epitope on Cre was performed on adjacent section after antigen retrieval.

(**C,D**) *C1ql3* cKO mice displayed no phenotype in the open field test or the elevated plus maze test.

(**E**) *C1ql3* cKO mice infected with WGA-Cre AAV had a reduction in both contextual and cued fear memory.

Data are means ± SEM; the number of mice analyzed is displayed in each graph. Statistical analysis was performed using repeated measures 2-way ANOVA with post-hoc Bonferroni's test. See also Fig. S6.

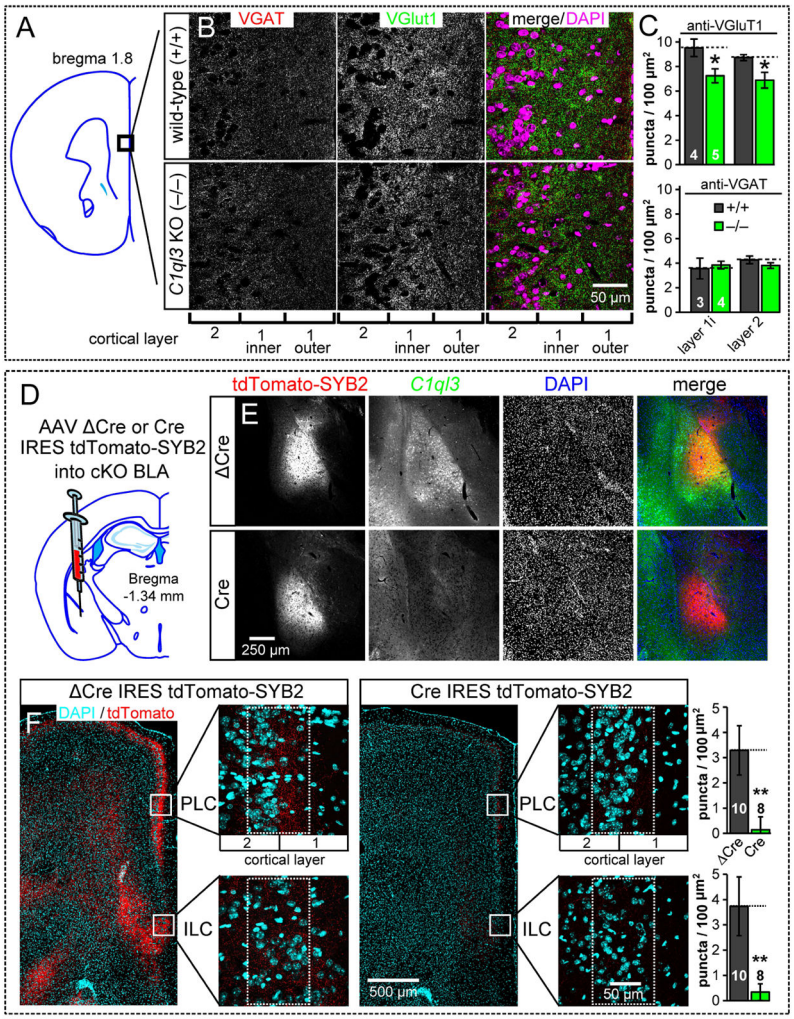

Fig. 7. Constitutive *C1ql3* KO decreases the excitatory synapse density in the mPFC, and conditional KO of *C1ql3* in the BLA nearly abolishes the synaptic projections formed by BLA neurons in the mPFC

(**A**) Diagram indicating the mPFC region analyzed.

(**B**) Representative images of mPFC cryosections from wild-type and KO mice stained for VGluT1, VGAT, and DAPI.

(**C**) Summary graphs of synaptic puncta density in wild-type and KO mPFC. Quantification areas were divided into the nuclei dense layer 2 and the inner half of the nuclei sparse layer 1 (layer 1i).

(**D**) Strategy for conditional KO of *C1ql3* in the BLA combined with anterograde targeting of tdTomato to mark presynaptic terminals. AAVs encoding ΔCre-IRES-tdTomato-SYB2 or Cre-IRES-tdTomato-SYB2 were injected into 9 week old mice; mice were analyzed 5 weeks later.

(**E**) Representative sections demonstrating the targeting of AAV to express tdTomato-SYB2 in the BLA and the absence of *C1ql3* expression in the BLA after expression of Cre.

(**F**) Representative sections (left) illustrating that conditional KO of *C1ql3* in the BLA causes nearly complete loss of presynaptic terminals projecting from the BLA to the mPFC.

Images show low-magnification overviews of the mPFC as well as high-magnification views of the PLC and ILC (boxed regions) from control mice (ΔCre AAV) and test mice (Cre AAV). Summary graphs (right) display the density of synaptic puncta in the PLC and ILC regions.

Data are means ± SEM; for (C) the number of mice analyzed is displayed in the graph; for (F) each AAV injected hemisphere was scored separately and the number of hemispheres analyzed is displayed in the graph. Statistical analyses were performed using Student's t-test. See also Fig. S7.

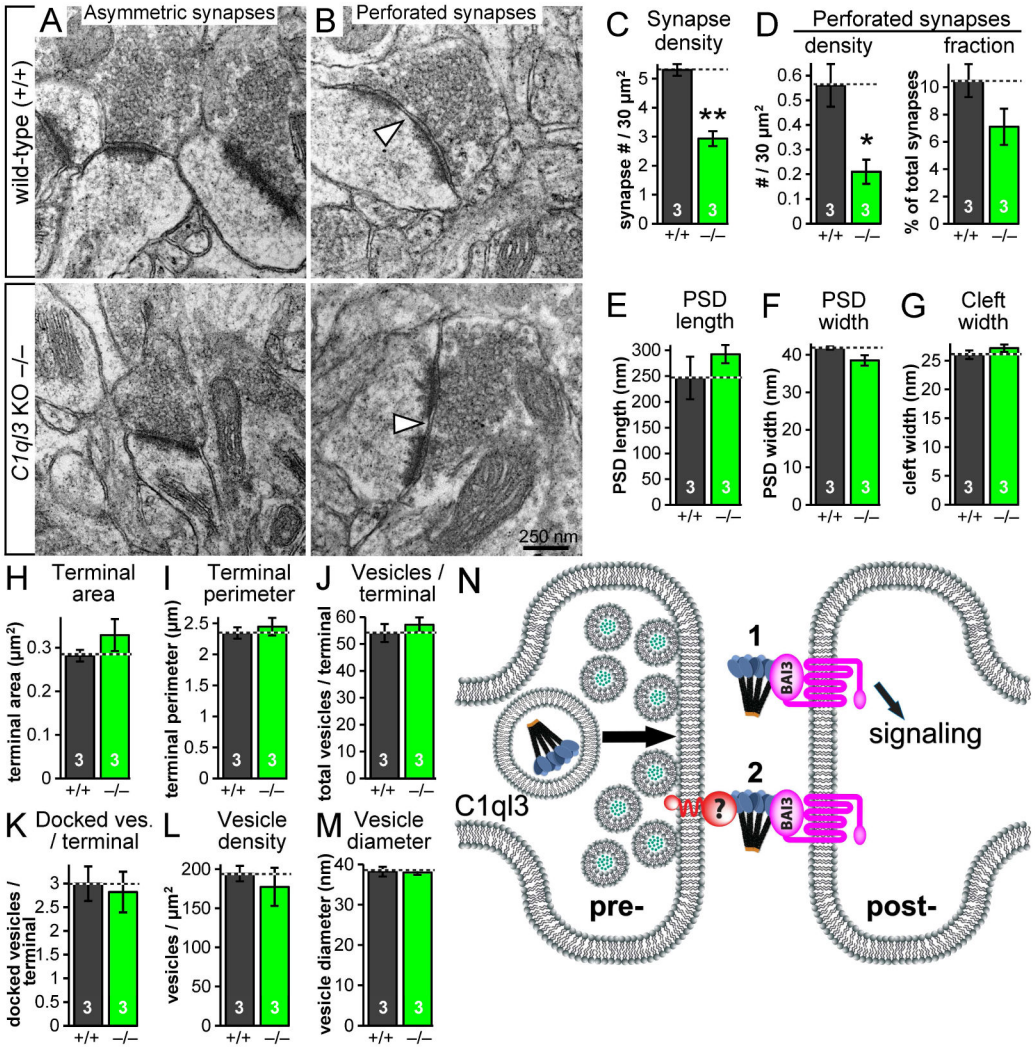

Fig. 8. Electron microscopy reveals that the *C1ql3* KO decreases asymmetric synapse density in the mPFC

(**A**) Representative images of asymmetric synapses in adult wild-type and KO PLC, focusing on the cortical layer 2/1 boundary.

(**B**) Representative images of perforated asymmetric synapses. Arrowheads point to the gap in the perforated postsynaptic density.

(**C**) Summary graph of the density of asymmetric synapses.

(**D**) Summary graphs of the density of perforated synapses, and fraction of total synapses that were perforated.

(**E–M**) Summary graphs of PSD length, PSD width, width of the synaptic cleft, presynaptic terminal area, presynaptic terminal perimeter, number of presynaptic vesicles per terminal, number of docked presynaptic vesicles per terminal, presynaptic vesicle density, and presynaptic vesicle diameter.

(**N**) Cartoon of two possible mechanisms for C1ql3's influence on synapses.

Data are means ± SEM; n = 3 mice. Statistical analyses were performed using Student's t-test.